AFRL-RX-WP-TP-2010-4073

MICROSTRUCTURAL EVOLUTION IN LASER DEPOSITED NICKEL-TITANIUM-CARBON IN SITU METAL-MATRIX COMPOSITES (Preprint)

J. Tiley

Metals Branch
Metals, Ceramics, and Nondestructive Evaluation Division

S. Gopagoni, A. R. P. Singh, J. Y. Hwang, T. W. Scharf, and, R. Banerjee

University of North Texas

JANUARY 2010
Interim Report

AIR FORCE RESEARCH LABORATORY
MATERIALS AND MANUFACTURING DIRECTORATE
WRIGHT-PATTERSON AIR FORCE BASE, OH 45433-7750
AIR FORCE MATERIEL COMMAND
UNITED STATES AIR FORCE

REPORT DOCUMENTATION PAGE

Form Approved
OMB No. 0704-0188

1. REPORT DATE *(DD-MM-YY)*	2. REPORT TYPE	3. DATES COVERED *(From - To)*
January 2010	Journal Article Preprint	01 January 2010 – 01 January 2010

4. TITLE AND SUBTITLE
MICROSTRUCTURAL EVOLUTION IN LASER DEPOSITED NICKEL-TITANIUM-CARBON IN SITU METAL-MATRIX COMPOSITES (Preprint)

5a. CONTRACT NUMBER
IN HOUSE

5b. GRANT NUMBER

5c. PROGRAM ELEMENT NUMBER
62102F

6. AUTHOR(S)
J. Tiley (Metals, Ceramics, and Nondestructive Evaluation Division, Metals Branch (AFRL/RXBM))
A. R. P. Singh, K. C. Mahdak, S. Gopagoni, J. Y. Hwang, S. Nag, and R. Banerjee (University of North Texas)

5d. PROJECT NUMBER
4347

5e. TASK NUMBER
RG

5f. WORK UNIT NUMBER
M02R1000

7. PERFORMING ORGANIZATION NAME(S) AND ADDRESS(ES)

Metals Branch (AFRL/RXBM)
Metals, Ceramics, and Nondestructive Evaluation Division
Materials and Manufacturing Directorate, Air Force Research Laboratory
Wright-Patterson Air Force Base, OH 45433-7750
Air Force Materiel Command, United States Air Force

University of North Texas
Center for Advanced Research and Technology and Department of Materials Science

8. PERFORMING ORGANIZATION REPORT NUMBER
AFRL-RX-WP-TP-2010-4073

9. SPONSORING/MONITORING AGENCY NAME(S) AND ADDRESS(ES)
Air Force Research Laboratory
Materials and Manufacturing Directorate
Wright-Patterson Air Force Base, OH 45433-7750
Air Force Materiel Command
United States Air Force

10. SPONSORING/MONITORING AGENCY ACRONYM(S)
AFRL/RXLM

11. SPONSORING/MONITORING AGENCY REPORT NUMBER(S)
AFRL-RX-WP-TP-2010-4073

12. DISTRIBUTION/AVAILABILITY STATEMENT
Approved for public release; distribution unlimited.

13. SUPPLEMENTARY NOTES
PAO case number 88 ABW-2009-5145, cleared 11 December 2009. This work was funded in whole or in part by Department of the Air Force work unit M02R1000. The U.S. Government has for itself and others acting on its behalf an unlimited, paid-up, nonexclusive, irrevocable worldwide license to use, modify, reproduce, release, perform, display, or disclose the work by or on behalf of the U. S. Government. Submitted to the Journal of Materials Science. Paper contains color.

14. ABSTRACT
Laser deposition of a mixture of elemental nickel, titanium, and carbon (graphite) powders with varying compositions, via the laser engineered net shaping (LENS) process, has resulted in novel in situ metal-matrix composites. The microstructure in these in situ composites can be substantially tailored depending on the ratio of graphitic carbon to titanium added. A lower C/Ti ratio results in a harder composite consisting of primary titanium carbide precipitates within a eutectic matrix consisting of nickel and titanium carbide while a higher C/Ti ratio results in a softer composite consisting of primary graphitic carbon bundles within the same type of eutectic matrix. These composites have been characterized in detail using x-ray diffraction, scanning electron microscopy (including energy dispersive spectroscopy mapping), and, transmission electron microscopy.

15. SUBJECT TERMS
laser deposition, elemental nickel, titanium, and carbon, scanning electron microscopy

16. SECURITY CLASSIFICATION OF:			17. LIMITATION OF ABSTRACT:	18. NUMBER OF PAGES	19a. NAME OF RESPONSIBLE PERSON (Monitor)
a. REPORT	b. ABSTRACT	c. THIS PAGE			Christopher F. Woodward
Unclassified	Unclassified	Unclassified	SAR	20	19b. TELEPHONE NUMBER *(Include Area Code)* N/A

Standard Form 298 (Rev. 8-98)
Prescribed by ANSI Std. Z39-18

Microstructural Evolution in Laser Deposited Nickel-Titanium-Carbon In Situ Metal-Matrix Composites

S. Gopagoni, A. R. P. Singh, J. Y. Hwang, T. W. Scharf, J. Tiley*, and, R. Banerjee

Center for Advanced Research and Technology and Department of Materials Science and Engineering, University of North Texas, Denton, Texas, U.S.A.

*Air Force Research Laboratory, Dayton, Ohio, U.S.A.

Abstract

Laser deposition of a mixture of elemental nickel, titanium, and carbon (graphite) powders with varying compositions, via the laser engineered net shaping (LENS) process, has resulted in novel in situ metal-matrix composites. The microstructure in these in situ composites can be substantially tailored depending on the ratio of graphitic carbon to titanium added. A lower C/Ti ratio results in a harder composite consisting of primary titanium carbide precipitates within a eutectic matrix consisting of nickel and titanium carbide while a higher C/Ti ratio results in a softer composite consisting of primary graphitic carbon bundles within the same type of eutectic matrix. These composites have been characterized in detail using x-ray diffraction, scanning electron microscopy (including energy dispersive spectroscopy mapping), and, transmission electron microscopy.

Introduction

Metal Matrix Composites (MMC) are used in several engineering applications including aerospace applications, due to their higher specific stiffness and strength, and, promising high temperature mechanical properties such as creep resistance. Various metals Al, Cu, Fe, Mg, Ti, Ni, etc are used as matrices with titanium carbide as the reinforcement phase since it has high hardness (2859-3200 HV), a high melting point (3067°C), a low density (4.93 g/cm^3), and high mechanical strength. Though titanium carbide (TiC) is very hard, it is extremely brittle, and consequently is used in engineering applications more as a reinforcement in a ductile and tough metal matrix (e.g. nickel) rather than as a monolithic ceramic. Furthermore, nickel and nickel-base superalloys are employed in a wide range of applications, including aircraft jet engines,

land-based turbines, chemical/petrochemical plants, and, are also important candidate alloys for the next generation of nuclear reactors. Nickel does not form an equilibrium carbide phase [hwang] and therefore, the combination of titanium carbides reinforcing a nickel or nickel-base matrix is very promising as a hybrid material for high temperature structural applications.

There have been some previous studies on nickel-titanium carbide composites, primarily focusing on different aspects of processing these composites [2]. Choi et al. [3] studied the densification behavior of the TiC_x- 50 wt% Ni composites processed via self- propagating high temperature synthesis (SHS). They reported that the densities of the liquid-phase sintered samples were greater than ~97% theoretical density whereas the liquid infiltrated sample was ~95%. Li et al. [4] investigated Ni-TiC composites processed by direct laser fabrication (DLF) from a feedstock of elemental nickel and titanium carbide powders. They focused on the influence of volume fraction of TiC on micro hardness and wear resistance of these composites and reported that increasing the volume fraction of TiC to 60%, resulted in an increase in the average size of the carbide precipitates, the micro-hardness, and, the wear resistance. Huang et. al. [5] investigated the microstructure of Ni-TiC composites processed by mechanical alloying (MA) of elemental Ni, Ti and C powders. The results of their study indicate that mechanical alloying resulted in both melting of powders and subsequent solidification by quenching, governed by a gradual SHS reaction. Takahashi [6] carried out differential thermal analysis (DTA) experiments coupled with microstructural analysis of the Ni- TiC system (5 – 90 wt% TiC) from room temperature to ~1400^{o}C and found that all the specimens exhibited an endothermic peak starting in the range 1284-1289^{o}C. However, additions of 5-20 wt% Mo, Ta, or Co changed the starting temperature for this endothermic reaction in the DTA analysis. In case of most previous studies on Ni-TiC composites, the volume fraction of the carbide phase has been relatively high resulting in the metallic nickel acting as a binder for the high volume fraction of ceramic particles. Furthermore, the carbide phase was introduced in these composites directly as TiC powder.

The present paper focuses on laser deposition of metal-matrix composites based on Ni-Ti-C using the laser engineered net shaping (LENS) process. The aim is to exploit the inherent rapid solidification rates in LENS processing to achieve a homogeneous distribution of titanium carbide precipitates reinforcing the nickel matrix, while maintaining the volume fraction of these

precipitates relatively low. Furthermore, the influence of changing the relative amounts of titanium and carbon (graphite) on the microstructure of these composites has also been investigated. The three salient features of the present investigation are listed below:

1. Laser deposition of Ni-TiC composites with a relatively low volume fraction of refined homogeneously distributed carbide precipitates.

2. Formation of in situ carbide precipitates due to the reaction between elemental titanium and carbon within molten nickel.

3. Controlling the microstructure in the laser deposited composites by tailoring the ratio of carbon to titanium (C/Ti ratio) in the composition to form both Ni+TiC as well as Ni+TiC+C(graphite) microstructures.

The mixture of a homogeneous distribution of refined hard carbide precipitates together with graphitic carbon in a nickel matrix is expected to offer an excellent combination of strength and stiffness together with lubricity in these composites.

Experimental Procedure

A commercial LENS 750 system, manufactured by Optomec Inc., was used for processing these composites. Similar to rapid prototyping technologies such as stereolithography, the LENS process begins with a computer-aided design (CAD) design file of a three-dimensional component, which is sliced into a series of layers electronically. The information about each of these layers is transmitted to the manufacturing assembly. The entire deposition is carried out inside a glove box with a controlled inert argon gas environment. The argon gas is continuously re-circulated during the LENS deposition process. A metal or alloy substrate is used as a base for depositing the component. A schematic diagram of the LENS system is shown in Fig. 1. In this case, a nickel plate substrate was used for depositing the Ni-Ti-C *in situ* composites. A high powered 500 W Nd:YAG laser, emitting near-infrared laser radiation at a wavelength of 1.064 μm (1064 nm), is focused on the substrate to create a melt pool into which the powder feedstock is delivered through an inert gas flowing through a multi-nozzle assembly. The nozzle is designed such that the powder streams converge at the same point on the focused laser beam.

Subsequently the substrate is moved relative to the laser beam on a computer-controlled stage to deposit thin layers of controlled width and thickness [7]. The energy density is typically maintained in the range of 30,000 to 100,000 W/cm^2. The oxygen content in the glove box was maintained below 10 ppm during all the depositions. The measured powder flow rate was 2.57 g/min while the argon volumetric flow rate was maintained at 3 litres/min. The scan speed of the Nd:YAG laser was 10 inches/min and the hatch width used for the depositions was 0.01 inches. The powders used for depositing the Ni-Ti-C composites consisted of commercially pure near-spherical Ni (40–150 μm) powders, pure Ti (40-150μm) and Ni coated graphite powders (all from Crucible Research^{TM}). Prior to deposition, the nickel, titanium and nickel coated graphite powders were pre-mixed in a twin-roller mixer. This mixing was carried out for 4 h, after which the powder was introduced into the power feeder of the LENS deposition system and the composites were laser deposited. These powders were mixed in three different ratios as listed in Table I. The composites were laser deposited in a cylindrical geometry of diameter 10 mm and height 10 mm. The laser power used in these depositions was 375 W. These LENS deposited in situ composites were characterized by scanning electron microscopy (SEM) in a FEI Quanta ESEM with a tungsten filament. The micro-hardness of these samples was determined using a standard Vickers micro-hardness tester. X-ray diffraction experiments were carried out in a Rigaku Ultima III diffractometer with a Cu Kα incident x-ray source. In addition, the LENS deposits were also characterized by transmission electron microscopy (TEM). 3mm diameter disc specimens were prepared from the LENS deposits using a combination of Electro-discharge Machining (EDM) and low-speed diamond saw sectioning. These discs were mechanically thinned using a series of abrasive papers starting from 600 grit upto 1200 grit. Subsequently, these discs were further mechanically thinned in a Gatan dimple grinder, and then ion-milled to electron transparency in a Gatan Duo Mill using 5 keV Ar ions. The TEM specimens were characterized in a FEI Tecnai F20 field-emission gun (FEG) TEM at an operating voltage of 200 keV.

Results & Discussion

Fig. 2 shows the x-ray diffraction (XRD) patterns for the three different Ni-Ti-C composites with different compositions (shown in Table I) and C/Ti ratios of 1, 2.98, and, 5.97 respectively. For

convenience the three different compositions will be referred to as Ni-10Ti-10C, Ni-7Ti-20C, and, Ni-3Ti-20C, respectively. The primary peaks in case of all three diffraction patterns can be consistently indexed based on the face-centered cubic (fcc) Ni phase and the δ-TiC phase exhibiting the rocksalt (NaCl-type) structure [8-9]. With increasing carbon content, and concomitant decrease in Ti content, the peaks arising from the δ-TiC phase appear to be progressively decreasing in relative intensity indicating a decrease in the volume fraction of this phase. In case of the Ni-10Ti-10C sample, the only peaks visible in the XRD pattern belong to the fcc Ni and δ-TiC phases. However, in case of both Ni-7Ti-20C and Ni-3Ti-20C, a carbon peak at $2\theta \sim 26°$, corresponding to the {0002} planes of graphite, is clearly visible with the intensity being higher in case of the Ni-3Ti-20C sample. The XRD data clearly indicates that increasing the C/Ti ratio results in a decrease in the δ-TiC phase and an increase in graphitic carbon in these composites. The same was confirmed by SEM analysis of these samples as shown in Fig. 3. Figs. 3(a) & (b) show backscatter SEM images of the Ni-10Ti-10C sample clearly exhibiting coarser and faceted primary carbide precipitates together with finer scale eutectic carbides, homogeneously distributed within the Ni matrix. Figs. 3(c) & (d) correspond to the Ni-7Ti-20C sample exhibiting bundles of dark contrast, in addition to the carbide precipitates. These dark bundles are likely to be the graphitic carbon phase identified in the XRD patterns. Finally, Figs. 3(e) & (f) correspond to the Ni-3Ti-20C sample and shows a higher volume fraction of graphitic bundles as compared to carbide precipitates presumably due to the substantially higher C/Ti ratio in this sample. Furthermore, as compared to the Ni-7Ti-20C sample, the Ni-3Ti-20C sample contains only refined eutectic carbide precipitates and hardly any coarser primary faceted carbide precipitates. Qualitative chemical analysis of these microstructures is shown in Fig. 4 where energy dispersive spectroscopy (EDS) maps corresponding to a representative region in the Ni-10Ti-10C sample have been plotted. The original backscatter SEM image is shown in Fig. 4(a) and the corresponding Ti, Ni, and, C EDS maps are shown in Figs. 4(b), (c), and, (d) respectively. All these four images are at exactly the same magnification. These EDS maps clearly reveal that the primary carbide precipitates are enriched in Ti, depleted in Ni, and, enriched in C. A higher magnification Ti EDS map, shown in Fig. 4(e), reveals the Ti enrichment in the finer scale eutectic carbide precipitates. Transmission electron microscopy (TEM) images and diffraction patterns from these Ni-Ti-C composites ae shown in Figs. 5 and 6. Fig. 5(a) shows a bright-field TEM image from the Ni-10Ti-10C sample

showing primary and eutectic carbide precipitates. Electron diffraction patterns from the primary carbide precipitates, shown in Figs. 5(b) and (c), can be consistently indexed as the [112] and [011] zone axes of the δ-TiC phase exhibiting a NaCl-type rocksalt structure. This is consistent with the results from the XRD patterns from the same sample. Electron diffraction patterns from the eutectic carbides also confirmed the same δ-TiC structure. TEM analysis of the Ni-3Ti-20C sample is shown in Fig. 6. A bright-field TEM image of the carbon-rich bundles is shown in Fig. 6(a) and a high-resolution TEM image revealing the internal structure within one of these bundles is shown in Fig. 6(b). Graphene layers are clearly visible in Fig. 6(b) confirming that these bundles are graphitic in nature and embedded within the Ni matrix of these composites. The electron diffraction, shown as an inset in Fig. 6(b), is further confirmation of the graphitic nature of these bundles. A bright-field TEM image of a eutectic carbide precipitate within the Ni matrix is shown in Fig. 6(c). Electron diffraction patterns from this eutectic carbide, not shown in this figure, confirmed the same δ-TiC structure in these precipitates.

Microhardness values for the three different laser-deposited composites are listed in Table I, with the relative values decreasing with increasing C/Ti ratio from Ni-10Ti-10C to Ni-7Ti-20C to Ni-3Ti-20C. The highest average microhardness value of 370 VHN was exhibited by the Ni-10Ti-10C sample. The decrease in microhardness with increasing C/Ti ratio is consistent with the microstructure results discussed previously. Thus, the greatest volume fraction of TiC precipitates is observed in case of the Ni-10Ti-10C sample and consequently this sample exhibits the highest hardness. The Ni-7Ti-20C sample exhibits a microstructure consisting of both primary and eutectic carbides as well as graphitic bundles. In contrast, the Ni-3Ti-20C sample with the greatest C/Ti ratio exhibits the least volume fraction of TiC precipitates and a relatively large volume fraction of graphitic bundles. Consequently, the Ni-7Ti-20C sample exhibits a microhardness of 290 VHN, that is greater than the value of 240 VHN exhibited by the Ni-3Ti-20C sample, but substantially lower than the 370 VHN microhardness exhibited by the Ni-10Ti-10C sample. Plotting the three compositions corresponding to the three composites on a ternary Ni-Ti-C phase diagram, shown in Fig. 7, leads to a better understanding of the phase stability and microstructure exhibited by these composites. Thus, as seen in Fig. 7, the Ni-10Ti-10C composition lies in the two-phase field, Ni + TiC, very close to the phase boundary between this

two-phase field and the Ni + C + TiC three-phase field. In contrast, the Ni-7Ti-20C and Ni-3Ti-20C compositions clearly lie within the Ni + C + TiC three-phase field. Consequently, the microstructures exhibited by these three compositions are consistent with their location on the ternary phase diagram. Based on this the sequence of phase formation for these three compositions can be determined as follows:

1. Ni-10Ti-10C: Liquid Ni (Ti,C) → Liquid Ni + Primary TiC → Primary TiC + Eutectic (Ni + TiC)
2. Ni-7Ti-20C: Liquid Ni (Ti,C) → Liquid Ni + Primary TiC + Primary C (graphite) → Primary TiC + Primary C (graphite) + Eutectic (Ni + TiC)
3. Ni-3Ti-20C: Liquid Ni (Ti,C) → Liquid Ni + Primary C (graphite) → Primary C (graphite) + Eutectic (Ni + TiC)

Summary and Conclusions

In situ composites of Ni-Ti-C with varying compositions have been deposited using the laser engineered net shaping (LENS) process. The C/Ti ratio can be used to tailor the microstructure and attendant properties of these in situ composites. Higher C/Ti ratio in case of the Ni-10Ti-10C composition leads to a hard composite exhibiting the formation of a large volume fraction of primary faceted TiC precipitates distributed within a eutectic Ni + TiC matrix. In contrast, a lower C/Ti ratio in case of the Ni-3Ti-20C composition leads to a substantially softer composite with a large volume fraction of primary graphitic carbon in the form of bundles distributed in a eutectic Ni + TiC matrix. However, the higher volume fraction of graphitic carbon could potentially be advantageous in improving the lubricity of these composites and consequently aid in achieving the appropriate balance between hardness and lubricity.

Acknowledgements

This work was financially supported by the U. S. Air Force Research Laboratory under contract FA8650-08-C-5226 (ISES contract). The authors also gratefully acknowledge the Center for Advanced Research and Technology (CART) at the University of North Texas.

References

1. J. Y. Hwang, A. Neira, T. W. Scharf, J. Tiley, and, R. Banerjee, *Scripta Mater*., **59**(5), 487 (2008).
2. Wang F, Mei J, Wu XH. Compositionally graded Ti6Al4V + TiC made by direct laser fabrication using powder and wire. Mater Design 2007; 28:2040-6.
3. Y. Choi, J. K. Lee, M. E. Mullins, *J. Mater. Sci* 32(1997) 1717-1724.
4. Yuxin Li, Peikang Bai, Yaomin Wang, Jiandong Hu, Zuoxing Guo. Mater Design 30(2009) 1409-1412
5. J. Y. Huang, L. L. YE, Y. K. Wu and H. Q. YE, Acta mater. Vol. 44, No. 5, pp 1781-1792, 1996.
6. S.Takahashi, S. Ikeno, E. Imai, JOM 16(1981) 3418-3426.
7. G.K. Lewis and E. Schlienger, Mater. Des. **21** (2000), pp. 417–423.
8. W. Lengauer, Transition metal carbides. nitrides and carbonitrides, in: R. Riedel (Ed.), Handbook of Ceramic Hard Materials, Vol. 1 Wiley–VCH, Weinheim, 2000, pp. 202–252.
9. F. Chien, S. Nutt, D. Cummings, Phil. Mag. A 68 (1993) 325

Tables

Sample	**Ti(at%)**	**C(at%)**	**Ni(at%)**	**Hardness(HV)**
Ni-10Ti-10C	**10.5**	**10.5**	**79**	**370 ± 10**
Ni-7Ti-20C	**6.6**	**19.7**	**73.7**	**290 ± 7**
Ni-3Ti-20C	**3.4**	**20.3**	**76.3**	**240 ± 6**

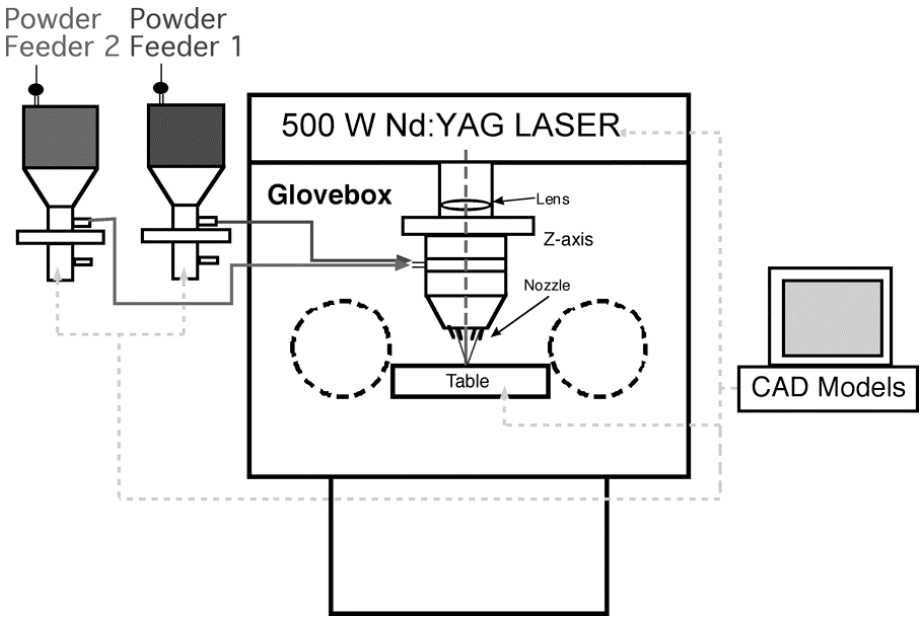
Powder Feeder 2
Powder Feeder 1
500 W Nd:YAG LASER
Glovebox
Lens
Z-axis
Nozzle
Table
CAD Models

Fig. 1.

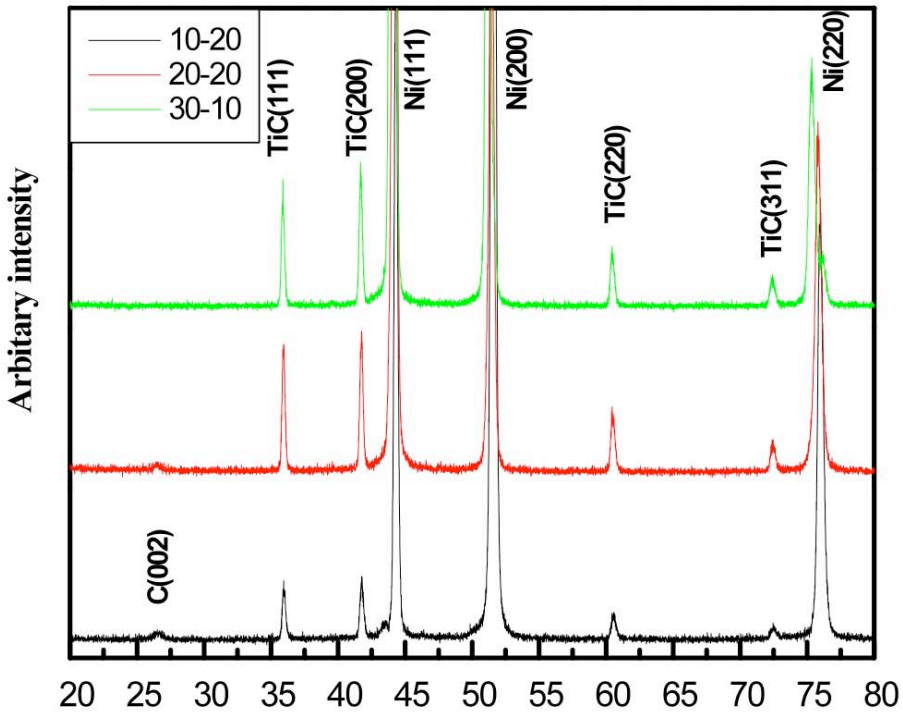
10-20
20-20
30-10
TiC(111)
TiC(200)
Ni(111)
Ni(200)
TiC(220)
TiC(311)
Ni(220)
C(002)
Arbitary intensity
20
25
30
35
40
45
50
55
60
65
70
75
80

Fig. 2.

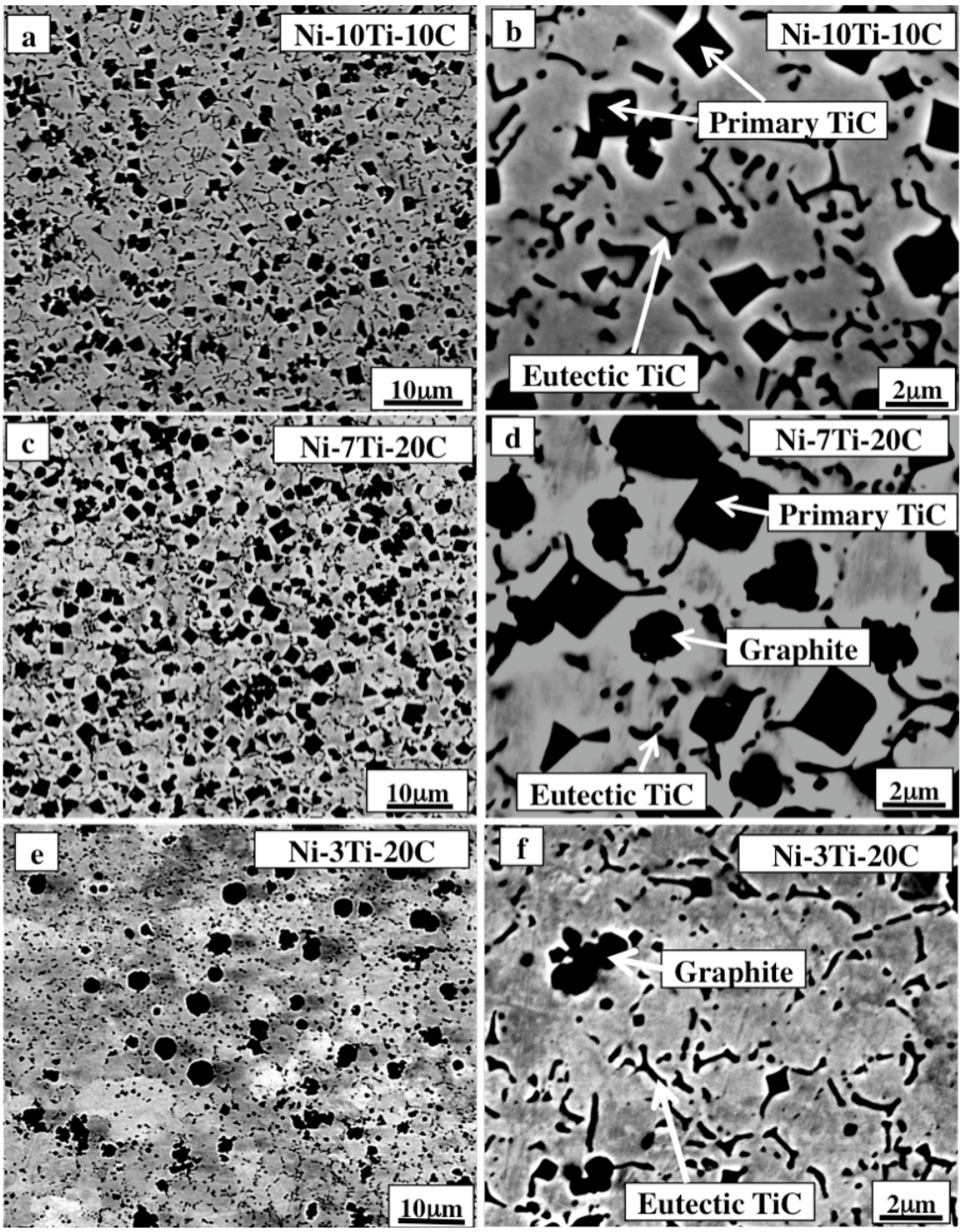
a
Ni-10Ti-10C
10μm
b
Ni-10Ti-10C
Primary TiC
Eutectic TiC
2μm
c
Ni-7Ti-20C
10μm
d
Ni-7Ti-20C
Primary TiC
Graphite
Eutectic TiC
2μm
e
Ni-3Ti-20C
10μm
f
Ni-3Ti-20C
Graphite
Eutectic TiC
2μm

Fig. 3.

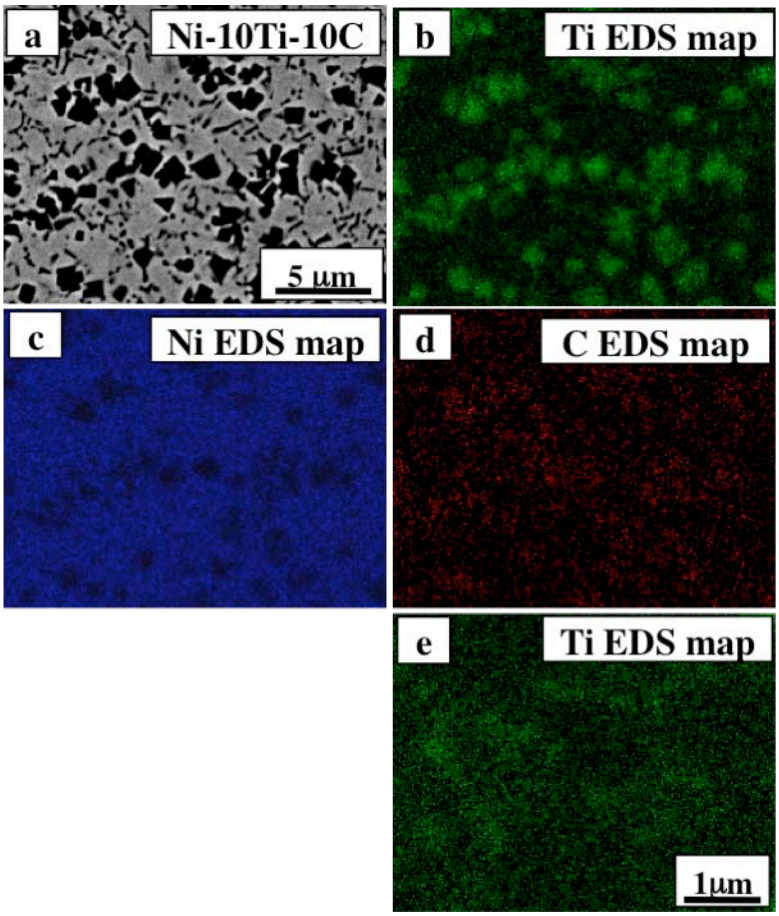
a
Ni-10Ti-10C
5 μm
b
Ti EDS map
c
Ni EDS map
d
C EDS map
e
Ti EDS map
1μm

Fig. 4.

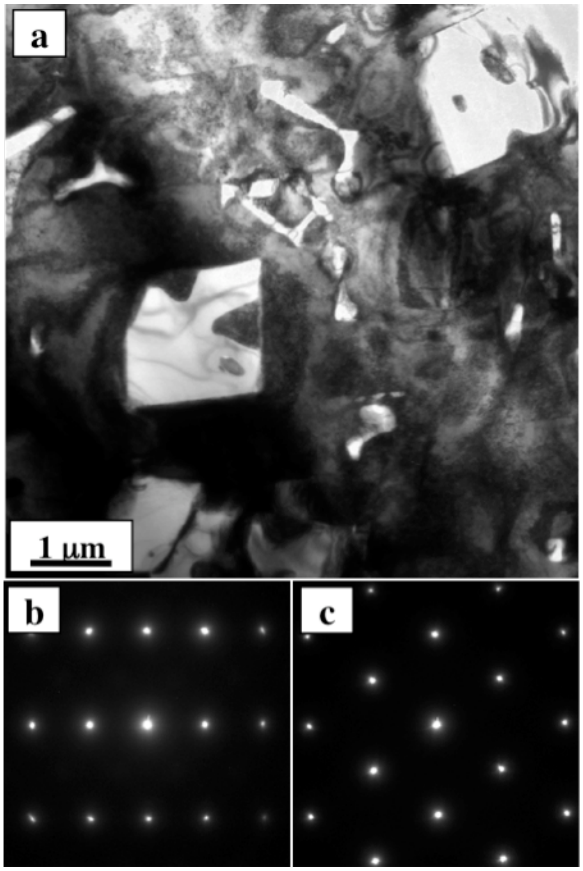

Fig. 5.

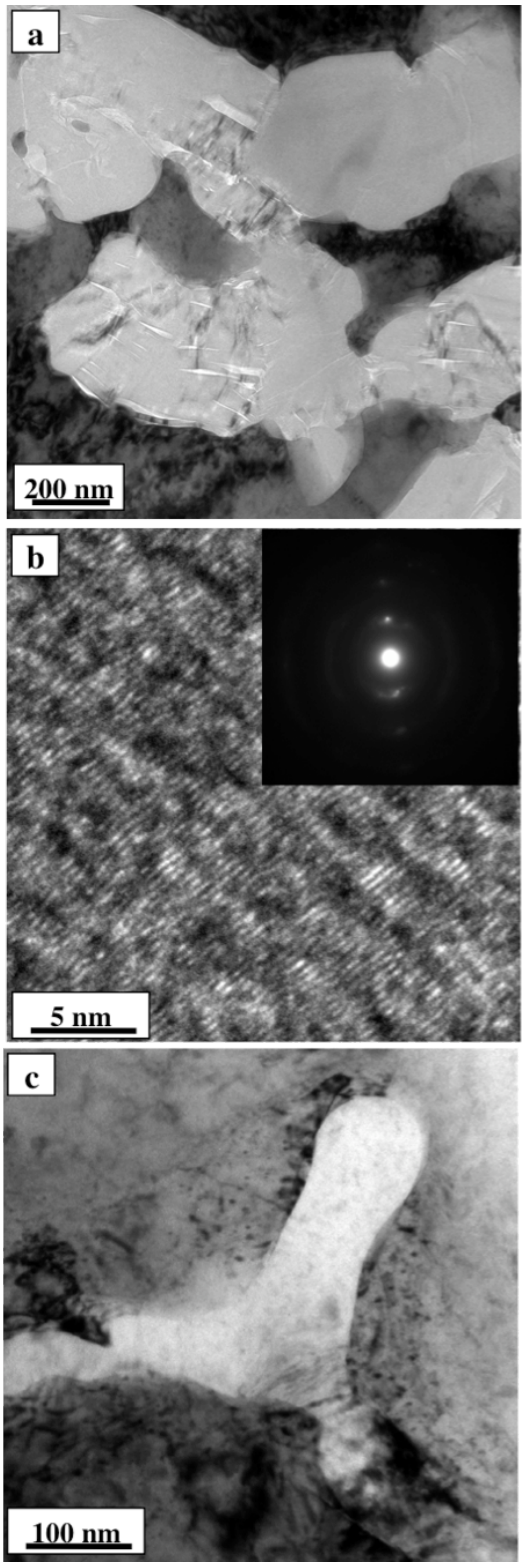

Fig. 6.

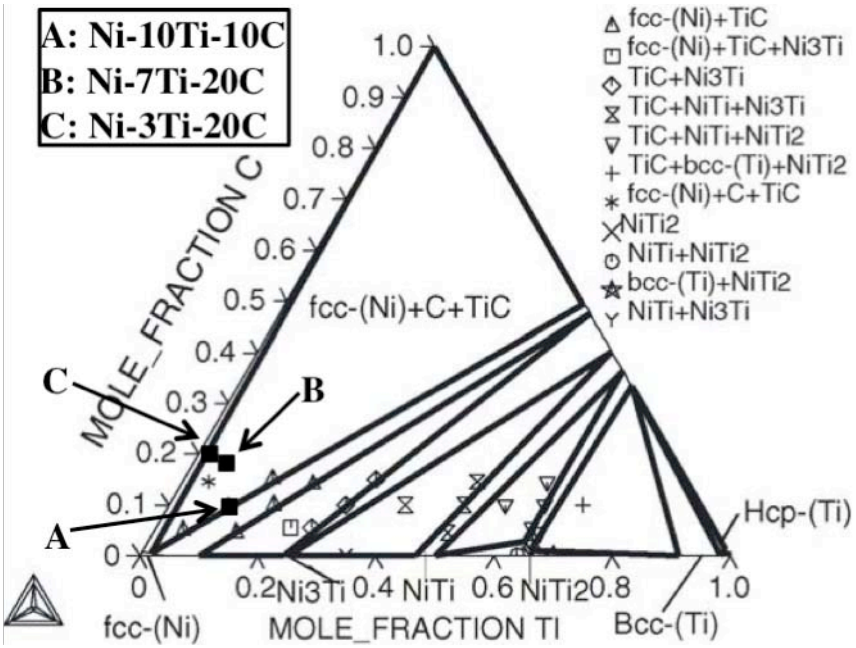
A: Ni-10Ti-10C
B: Ni-7Ti-20C
C: Ni-3Ti-20C
fcc-(Ni)+TiC
fcc-(Ni)+TiC+Ni3Ti
TiC+Ni3Ti
TiC+NiTi+Ni3Ti
TiC+NiTi+NiTi2
TiC+bcc-(Ti)+NiTi2
fcc-(Ni)+C+TiC
NiTi2
NiTi+NiTi2
bcc-(Ti)+NiTi2
NiTi+Ni3Ti
MOLE_FRACTION C
fcc-(Ni)+C+TiC
C
B
A
Hcp-(Ti)
0
0.1
0.2
0.3
0.4
0.5
0.6
0.7
0.8
0.9
1.0
0
0.2 Ni3Ti
0.4 NiTi
0.6 NiTi2
0.8
1.0
fcc-(Ni)
MOLE_FRACTION TI
Bcc-(Ti)

Fig. 7.